

Thickness Effects on Thin Film Gas Barriers: Silicon-Based Coatings

J.T. Felts, Airco Coating Technology

Keywords: SiO_x films; Permeation barrier coatings

ABSTRACT

High barrier, silicon-based, thin film layers were deposited onto poly(ethylene terephthalate) (PET) substrates with the QLF® coating process. The deposited SiO_x coating, unlike conventional polymeric barrier materials, did not have a predictable relationship between thickness and gas barrier properties. The features of the barrier performance/thickness curves are presented.

I. INTRODUCTION

Thin film transparent gas barriers are now widely discussed in the plastics packaging industry¹. Unfortunately, there are few examples of commercial products, none of which are cost competitive with polymeric materials. The road to cost competitiveness for existing technologies is paved with a solid understanding of the mechanisms that affect gas barrier and the means of measuring and controlling these mechanisms. This paper will discuss coating thickness and its effect on the oxygen transmission rate for poly(ethylene terephthalate) (PET) coated with SiO_x by evaporation and plasma processing.

II. EXPERIMENTAL

A plasma enhanced chemical vapor deposition process developed at Airco Coating Technology was used to produce QLF (quartz-like film) barrier coatings.²⁻⁴ The QLF depositions did not use silane, thus eliminating the associated gas handling issues (silane is highly pyrophoric). Instead an organosilicon source, tetramethyldisiloxane (TMDSO), was used. The QLF coatings were SiO_x (with x greater than 1.7), amorphous, highly inorganic, optically clear, well adhering (without surface pre-treatment), and required thicknesses of less than 600 Å to achieve the desired gas barrier properties. The QLF depositions took place at lower pressures (0.01-0.05 Torr) than those used in conventional PECVD. Even at the low processing pressure, the base pressure requirements before processing were loosened since high gas flows were used to displace contaminants.

A research roll-to-roll system was developed for QLF coating depositions (**Figure 1**). The Airco Coating Technology ILS-1600, used for the original development of the QLF coating technology, was modified to accommodate rolls of 12" wide, 12 micron thick PET up to 1000 feet in length. The web was not cooled since it "free-spanned" the process chamber, and the process thermal load was very low. Coupon samples (6" x 6") were also coated in a static mode. In all QLF depositions, the substrate was not intentionally cleaned or pre-treated prior to applying the SiO_x thin film.

The oxygen transmission rate was measured for appropriately coated 0.5 mil thick PET (ICI Melinex Type S and Hoechst Celanese Hostaphan 2400) with MOCON Controls, Inc. Ox-Tran equipment. Sample sizes of 50 and 100 cm² were measured. All values are reported in cc/100in²/day and were taken at 23°C and 75% relative humidity.

III. RESULTS

Table 1 lists the results from multiple QLF coating experiments. The QLF coating thickness in Table 1 was calculated from known deposition rates and deposition exposure times. The QLF coating thicknesses are considered to be within 10% of the actual absolute thickness as determined by TEM analysis of several samples.

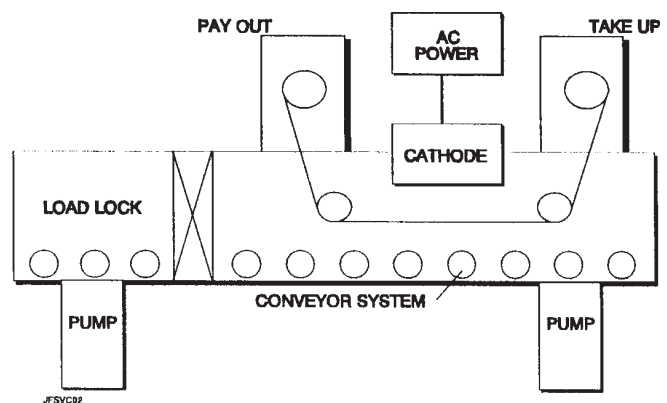


Figure 1 - Airco Coating Technology - ILS 1600

Table 1 - QLF @Barrier Coatings

	EXP#	OXTRAN (cc/100in ² /day)	Calc Thick (Å)	1/OXTRAN (cc/100in ² /day) ⁻¹
1	120889-1-2	2.58	75	0.388
2	900316-2-1	1.59	100	0.629
3	900316-2-2	0.23	150	4.348
4	120889-1-3	0.30	150	3.333
5	900316-2-3	0.05	200	20.000
6	120889-1-4	0.04	300	25.000
7	900316-2-4	0.04	300	25.000
8	PRO12690-4	0.04	510	25.000
9	PRO12990-1	0.03	558	33.333
10	PRO12990-1	0.02	650	50.000
11	102087-6	1.81	1969	0.552
12	102087-6	1.24	2851	0.806
13	020388-2	1.31	3278	0.763

IV. DISCUSSION

Conventional polymeric barrier materials have a constant bulk permeability (P) expressed in cc-mil/100in²/day, hence the gas transmission rate varies as the inverse of the thickness of the material:

$$P = \frac{P}{t} \quad (1)$$

where p is the permeance (cc/100in²/day) measured with the MOCON Controls equipment, P is permeability (cc-mil/100in²/day) and t is the thickness of the material in mils. For example, a Saran™ barrier material has an oxygen permeability (P_{O₂}) of 0.08 cc-mil/100in²/day, while polycarbonate has P_{O₂} = 300 cc-mil/100in²/day (data quoted are representative — suppliers should be consulted for currently available data). The permeability is proportional to the measured oxygen transmission or permeance (Figures 2-3), and the response function of the oxygen transmission to thickness is identical for each polymer, the magnitude reflecting the propensity of the material to retard the specific gas from diffusing. When different polymers

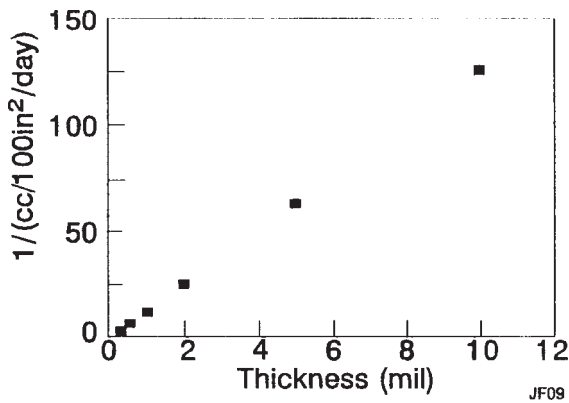


Figure 2 - Saran™

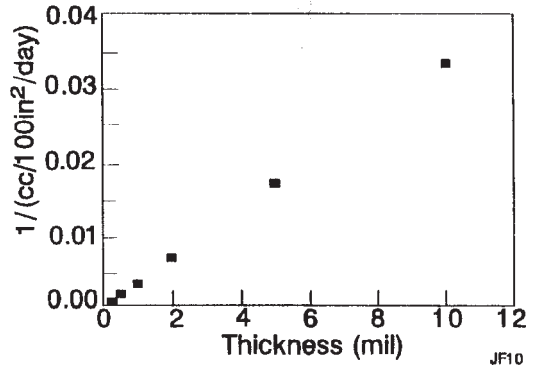


Figure 3 - Polycarbonate

are joined together to form a single material, the permeance of the composite multi-layer structure is found by adding the conductances in parallel:

$$Plaminate = \left[\left(\frac{t_1}{P_1} \right) + \left(\frac{t_2}{P_2} \right) + \left(\frac{t_n}{P_n} \right) \right]^{-1} \quad (2)$$

where Plaminate is the permeance of the total structure in cc/100in²/day and t_n denotes the thickness in mils of material n with permeability P_n in cc-mil/100in²/day. Using Equation 2, if 0.5 mils (t₁) of Saran (P₁ = 0.08 cc-mil/100in²/day) is combined with 20 mils (t₂) of polycarbonate (P₂ = 300 cc-mil/100in²/day), the resulting two layer composite structure gives plaminate = 0.16 cc/100in²/day permeance to oxygen. The relationship between the composite transmission rate and the layer thicknesses in multi-layer structures is not as simple as the single layer case above. Plotting the effect of polycarbonate thickness for a constant Saran thickness (0.5 mil), and the inverse, the effect of Saran thickness for a constant polycarbonate thickness (10 mils) yielded Figures 4-5. The polymer that had poor barrier to oxygen did not affect the laminates performance while the good barrier dominated the resulting permeance. Furthermore, the resulting thickness versus permeance plots reflect the materials' ability to enhance the overall structure and default to the single layer case if P₁ > P₂ and the thickness of layer 1 (t₁) is varied. When P₁ > P₂ and t₂ is varied the resulting two layer structure shows no change in its permeance (Figure 4).

In contrast to the polymer case, SiO_x coatings have a complex relationship between their thickness and resulting oxygen transmission (Table 1 and Figure 6). We believe this is due to both the growth mechanisms and the effect of the base polymeric material on the coating.⁵ During the nucleation of the QLF film (Area 1 of Figure 6), the extent of the PET surface coverage increased from 0% (no coating) to 100% as the QLF coating thickness increased from approximately 0-200Å,

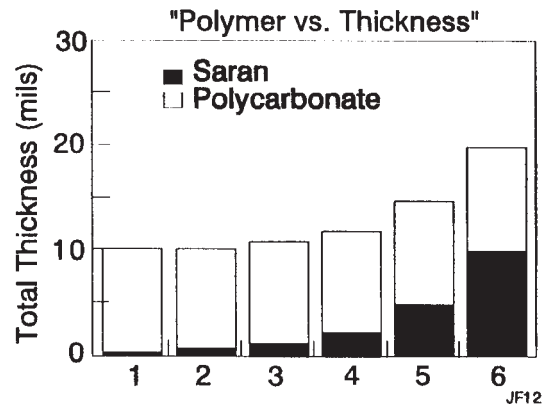
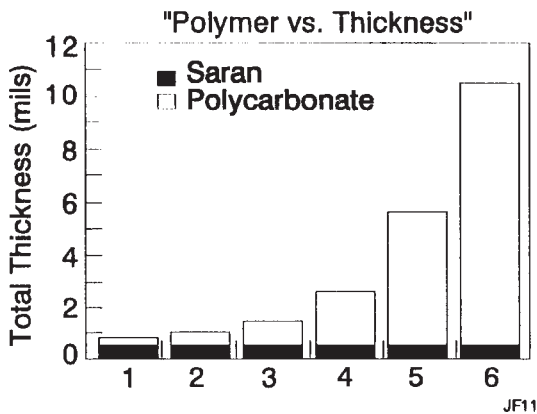
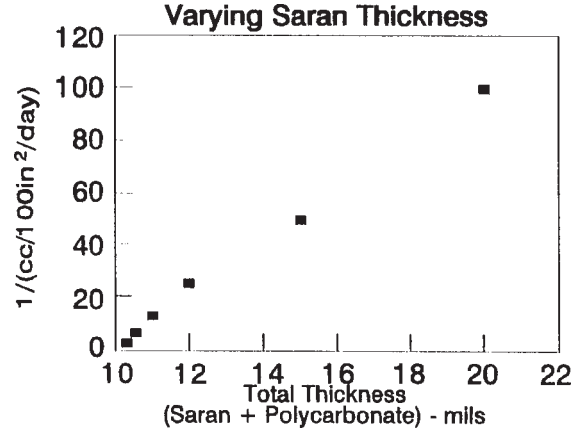
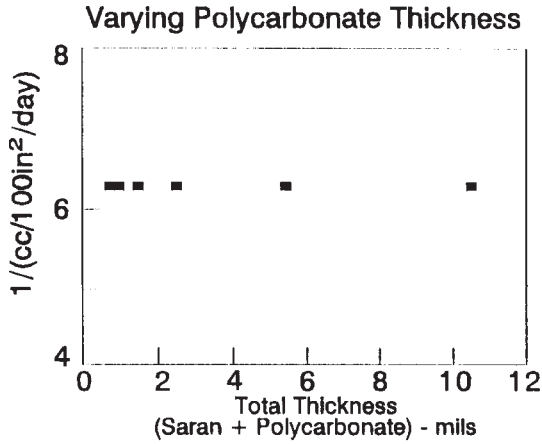


Figure 4 - Varying Polycarbonate Thickness Effects on Oxygen Transmission

Figure 5 - Varying Saran Thickness Effects on Oxygen Transmission

therefore the QLF permeance is a measure of the surface coverage of the PET. As the QLF coating thickness increased, the response of the composite was significantly different than the polymeric examples (Figure 7a).

As the coating thickness increased past 200Å (Area 1), the barrier performance of the coating did not improve significantly (Area 2 of Figure 6). The additional thickness of Area 2 had less of an effect on the actual transmission rate than the nucleation process of Area 1. In Area 2, the QLF coating/PET composite duplicates the two-layer case where $P_{SiO_x} > P_{PET}$ and t_{SiO_x} is varied (Figure 7b).

As the coating became thicker (Area 3, Figure 6), the permeance increased and the barrier performance deteriorated. Degradation of SiO_x coatings can be attributed to prolonged exposure of the PET substrates to the plasma, free-spanning of the web, and the inherent attributes of the SiO_x material as its bulk thickness is increased (such as internal stress being

released through cracking). Regardless of the mechanism, Area 3 does not follow the expected trend of Equation 2 (Figure 7c).

Applying Equation 2 above and solving for P_1 for a two-layer structure gives:

$$P_1 = \frac{P_{laminar} \times t_1}{[(1 - P_{laminar} \times t_2)/P_2]} \quad (3)$$

The permeability of the QLF coatings was calculated for each thickness in the above example (Table 2). The permeance of the base 0.5 mil PET was determined internally on MOCON equipment to be 7.77 cc/100in²/day (P_2/t_2). In Area 1 of Figure 6, the permeability of the QLF coating changed due to the changes in the conformal coverage of the substrate (Figure 8).

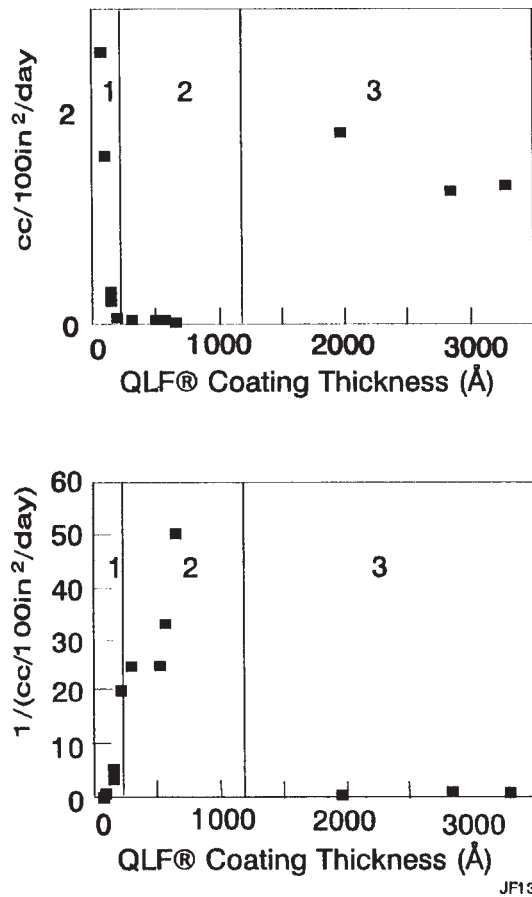


Figure 6 - QLF® Coating Oxygen Permeance

After the entire PET surface was coated, representing the processes' optimal thickness (Area 2), the permeability reached a semi-static value of 5.22×10^{-9} cc-mil/100in²/day (standard deviation = 2.11×10^{-9} for N=5) (Figure 8). The thickness increased in Area 2 and since the permeability was constant, the permeance followed the expected trend.

Area 3 can be thought of as the inverse of Area 1, decreasing the coatings surface coverage of the substrate. The decrease could be manifested by cracking (due to web handling), internal stresses of the SiO_x coating and/or thermal degradation of the PET and SiO_x. Areas 1 and 3 are independent of the theories detailed in equations 1-3 above and are dependent on the nature of the deposition process, specifically the thermal properties and growth mechanism. Only thermal effects are considered here since handling issues were consistent from experiment to experiment, and cracking and stress can be related to the thermal load of the process.

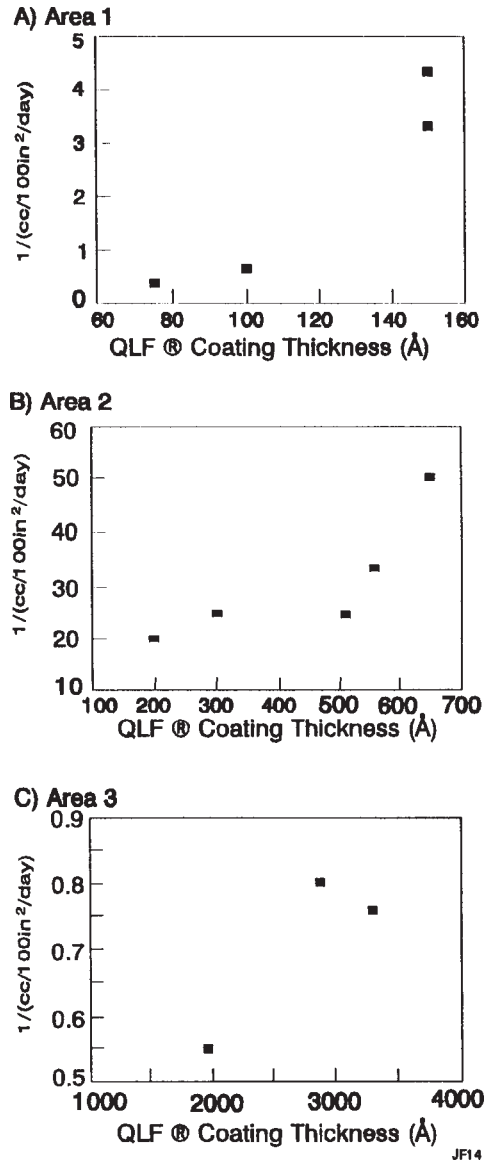


Figure 7 - QLF® Coating Oxygen Permeance

Table 2 - QLF® Barrier Coatings

AREA	OxTRAN cc/100in ² /day	Thickness (Å)	Thick (mils)	Permeability cc-mil/100in ² /day
I	2.58	75	2.95×10^{-08}	1.14×10^{-07}
	1.59	100	3.93×10^{-08}	7.86×10^{-08}
	0.30	150	5.90×10^{-08}	1.84×10^{-08}
	0.23	150	5.90×10^{-08}	1.40×10^{-08}
II	0.05	200	7.86×10^{-08}	3.96×10^{-09}
	0.04	300	1.18×10^{-07}	4.74×10^{-09}
	0.04	300	1.18×10^{-07}	4.74×10^{-09}
	0.02	350	1.38×10^{-07}	2.76×10^{-09}
	0.04	510	2.00×10^{-07}	8.06×10^{-09}
	0.03	558	2.19×10^{-07}	6.60×10^{-09}
	1.81	1969	7.74×10^{-07}	1.83×10^{-06}
III	1.24	2851	1.12×10^{-06}	1.65×10^{-06}
	1.31	3278	1.29×10^{-06}	2.03×10^{-06}

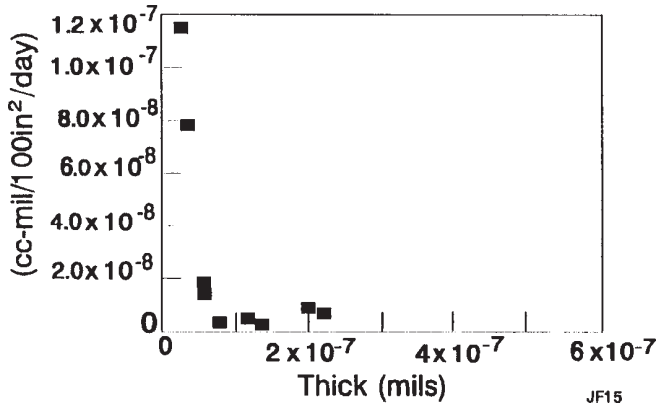


Figure 8 -QLF Oxygen Permeability

Previously published evaporation work has also demonstrated the thickness/permeance relationship seen with QLF coatings (Table 3 and Figure 9).⁶ In Area 1 the coating was nucleating and the permeability changed along with thickness. Due to the lack of data, Area 2 is not as well defined as in the QLF coating case, however, and could be smeared into the failure mode of Area 3. It is interesting to note the significant difference in permeabilities in Area 2 between QLF coatings and the evaporated SiO_x (5.33 x 10⁻⁸ cc-mil/100in²/day, sigma = 1.63 x 10⁻⁸, N = 5) material. The general shape of Area 2 is also interesting, showing the potential onset of permeance failure at much lower thicknesses for the evaporated films than for the plasma processed, QLF coatings. The differences in Areas 1 and 2 of Figures 6 and 9 are due to the way that the coatings grew and

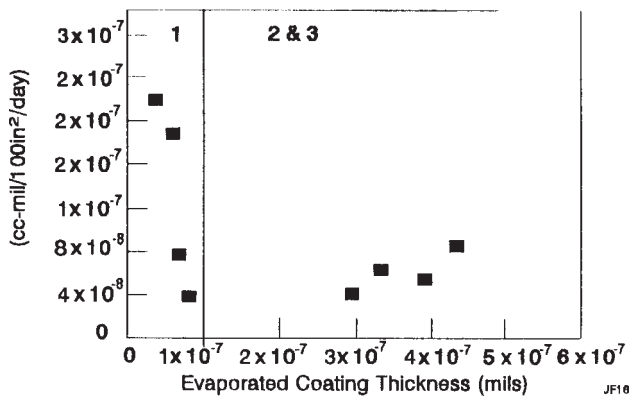


Figure 9 - Evaporated Oxygen Permeability Data

the plasma exposure that they received during the nucleation process as shown previously.⁵ Area 3 differences are due primarily to thermal effects of the process, since evaporation processes impart significantly more thermal energy into the substrate than the QLF coating process as demonstrated by the requirement for backside cooling in evaporation. Thickness is also related to thermal load, thicker coatings result in larger thermal loads than thin coatings. It is postulated that if the thermal load is increased beyond the evaporation curve (Figure 9), the permeability vs. thickness curve would collapse to a steep “V” shape, and the ultimate permeability achieved in Area 2 would increase significantly. This implies that by plotting the permeability versus thickness curve of the respective process, the optimal coating thickness (the intersection of Area 1 and Area 2), the sensitivity of the coating to failure due to increased thickness (or thermal load), and the absolute barrier achievable with any given deposition technology could be determined.

Table 3 - Evaporated SiO_x Data

OXTRAN (cc/100in ² /day)	Thickness (Å)	Thick (mils)	Permeability cc-mil/100in ² /day
3.23	100	3.93 x 10 ⁻⁰⁸	2.18 x 10 ⁻⁰⁷
2.26	150	5.90 x 10 ⁻⁰⁸	1.88 x 10 ⁻⁰⁷
0.97	175	6.88 x 10 ⁻⁰⁸	7.63 x 10 ⁻⁰⁸
0.45	200	7.86 x 10 ⁻⁰⁸	3.75 x 10 ⁻⁰⁸
0.13	750	2.96 x 10 ⁻⁰⁷	3.90 x 10 ⁻⁰⁸
0.18	850	3.34 x 10 ⁻⁰⁷	6.16 x 10 ⁻⁰⁸
0.13	1000	3.93 x 10 ⁻⁰⁷	5.20 x 10 ⁻⁰⁸
0.19	1100	4.32 x 10 ⁻⁰⁷	8.42 x 10 ⁻⁰⁸

The above model also explains why SiO_{1.5} coatings have shown superior performance over evaporated SiO₂ depositions. The heat of formation, of oxides of silicon increases as the stoichiometric point is reached. This is shown clearly by the difference between SiO (24 kcal/g-mole) and silicon dioxide (H_f = -205.4 kcal/g-mole).⁶ SiO_{1.5} would fall somewhere between SiO and SiO₂, therefore, the thermal load of SiO₂ will be much higher on the polymer web than SiO_x, where x < 2, when formed from oxygen addition to the SiO evaporation process. This phenomena was extrapolated in a previous paper (Figure 10).⁷⁶ The thermal load model may also explain why the SiO_{1.5} coatings are so highly variable, since the thermal energy imparted to the evaporated flux will vary strongly over the life of the evaporation crucible, and will depend highly on the relationship between the amount of evaporant and power applied. This implies that low temperature processes will provide the highest barrier and lowest variability over a given thickness range. It also suggests that

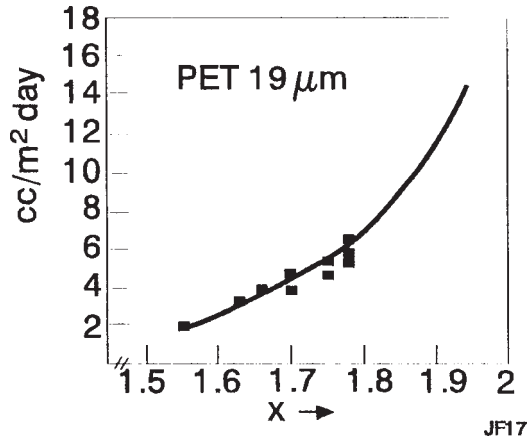


Figure 10 - Oxygen permeation vs. x of SiO_x -coated PET

only low temperature processes will result in thin high barrier (low P) coatings.

V. CONCLUSIONS

The thickness versus permeance curves of SiO_x coatings are significantly different than those for polymeric materials. The thin film SiO_x examples on PET substrates show three distinct phenomena. Area 1 of this relationship is due to the SiO_x nucleation process and the increases in PET surface coverage. Once an optimal thickness is reached (Area 2), the materials behave like their polymeric counterpart with constant permeability. After a critical thickness is reached, how-

ever, the permeance actually decreases (Area 3), and again the permeability changes. The thickness/permeance curves suggest that the thermal load of the particular process is a significant factor in determining the optimal thickness, absolute barrier achievable, and the stability of the coating process.

VI. ACKNOWLEDGMENTS

The author wishes to thank Dr. Hood Chatham and Robert Nelson for the many conversations that led to this paper.

VII. REFERENCES

1. J. Felts, "Advanced Materials: Solutions for the 90's", Proceedings from Enviroplas '90, Sept. 12-13, 1990, The Drake Hotel, Chicago, Ill.
2. E. Lopata and J. Felts, "Method of Plasma Enhanced Silicon Dioxide Deposition", European Patent Office, Publication #0299754 A2.
3. J. Felts and E. Lopata, "Plasma Thin Film Deposition Process Control", US Patent #4,888,199, Dec. 19, 1989.
4. J. Felts, J. Hofmann, and R. Hoffman, "Controlled Flow Vaporizer", US Patent #4,847,469, July 11, 1989.
5. J. Felts, Society of Vacuum Coaters 33rd Annual Technical Conference Proceedings, April 29- May 4, 1990, pp. 184-193.
6. Handbook of Chemistry and Physics, 60th Edition, Chemical Rubber Publishing Company 1981, p. D-75
7. T. Krug, Society of Vacuum Coaters 33rd Annual Technical Conference Proceedings, April 29- May 4, 1990, pp. 163-169.